

Recombination Radiation from InSb†

J. PEHEK* AND H. LEVINSTEIN

Department of Physics, Syracuse University, Syracuse, New York

(Received 7 May 1965)

The recombination radiation spectra of a variety of *n*- and *p*-type InSb single crystals were experimentally investigated at 300, 200, 100, and 12°K using radiation from a zirconium arc source as the generator of excess carriers. The emission spectra included contributions from direct band-to-band transitions, indirect phonon-assisted band-to-band transitions, transitions to flaws, and transitions between localized states not thermally coupled to the lattice, the transition energies of which were larger than the band gap of InSb. The direct band-to-band line, generally the major component, is in good agreement with the band model of this semiconductor. The room-temperature emission and radiative lifetime agree very well with those predicted by small-signal statistical theory. At 12°K a line at 0.215 eV is a result of an indirect band-to-band transition involving the emission of an optical phonon. Other lines in the 12°K spectra are correlated with the presence of zinc (0.228 eV), silver (0.209 and 0.186 eV), and gold (0.193 eV) as impurities. The energies of these emission lines indicate that at low concentrations the zinc level is 0.010 eV above the valence band, the two silver levels are located 0.027 eV and 0.050 eV above the valence band, and the lowest gold level is 0.043 eV above the valence band. One other line having no apparent relation to an impurity was observed at 0.225 eV. Emission from a highly impure *n*-type crystal revealed a decrease of the band gap due to the extension of the density-of-states below the intrinsic conduction band minimum and a rigid shift of the bands. Comparison of this experimental distribution with those calculated for band-to-band and band-to-flaw transitions from a filled band with and without *k* conservation indicate that in this case the emission is probably due to direct, non-*k*-conserving transitions. Narrow ($<kT$), low-intensity lines were superimposed upon the direct band-to-band radiative recombination photon distribution. Close to the energy of the band gap, these lines were equally spaced in energy (at about 0.010 eV). At higher energies the energy separation of these lines increased. The existence of these lines appears to be related to the concentration of electrons in the conduction band.

INTRODUCTION

THE study of radiative recombination in semiconductors has not only led to the development in recent years of highly efficient injection lasers and luminescent diodes, but has also yielded significant knowledge of the band structure, defect states, and recombination processes in many semiconducting materials. For such studies excess carrier populations have been generated by carrier injection across *p-n* junctions, photoexcitation by high-intensity sources, or electron-beam bombardment. The spontaneous recombination radiation in InSb has been studied to a certain extent using the first two methods of carrier generation.¹⁻³ Stimulated emission in InSb has been observed by electrical injection,⁴⁻⁷ electron bombardment,⁸ and most recently by optical injection.⁹

The study by Guillaume and Lavallard via electrical injection yielded highly resolved spectral data at 4, 77, and 300°K. Besides emission due to direct band-to-band transitions, they observed emission due to indirect band-to-band and band-to-flaw recombination. Moss, using radiation from a tungsten lamp to generate excess carriers, studied the room-temperature emission of InSb. The emission he observed, the result of band-to-band processes, agreed reasonably well with small signal theory.^{10,11} His data indicated that the room-temperature bulk-to-radiative lifetime ratio τ_B/τ_R was 0.21. However, subsequent lifetime studies^{12,13} fix the ratio of the measured room-temperature bulk lifetime to the calculated room temperature radiative lifetime (0.62 μ sec for intrinsic material) at about 7×10^{-2} . Mooradian and Fan, using both photo and electrical excitation, observed emission at low temperatures due to direct electron-hole recombination and transitions to an impurity level.

The experimental study which is the subject of this paper was concerned with a detailed study of radiative recombination in InSb upon optical injection. Emission was observed which is a result of both direct and in-

† This work has been supported by the Air Force Avionics Laboratory, Research and Technology, Air Force Systems Command, U. S. Air Force.

* Now at RCA Laboratories, Princeton, New Jersey.

¹ C. Benoit a la Guillaume and P. Lavallard, in *Proceedings of the International Conference on the Physics of Semiconductors, Exeter*, edited by A. C. Strickland (Institute of Physics and Physical Society, London, 1962), p. 875.

² T. S. Moss, *Proc. Phys. Soc. (London)* **B70**, 247 (1957).

³ A. Mooradian and H. Y. Fan, *Bull. Am. Phys. Soc.* **10**, 369 (1965).

⁴ R. J. Phelan, A. R. Calawa, R. H. Rediker, R. J. Keyes, and B. Lax, *Appl. Phys. Letters* **3**, 143 (1963).

⁵ B. L. Bell and K. T. Rogers, *Appl. Phys. Letters* **5**, 9 (1964).

⁶ M. Bernard, C. Chipaux, G. Duraffourg, M. Jean-Louis, J. Loudette, and J. Noblanc, *Compt. Rend.* **257**, 2984 (1963).

⁷ C. Benoit a la Guillaume and P. Lavallard, *Solid State Comm.* **1**, 148 (1963).

⁸ C. Benoit a la Guillaume and J. M. Debever, in *Symposium on Radiative Recombination in Semiconductors*, Paris, 1964

(unpublished); C. E. Hurwitz and R. J. Keyes, *Appl. Phys. Letters* **5**, 139 (1964).

⁹ R. J. Phelan, Jr., and R. H. Rediker, *Appl. Phys. Letters* **6**, 70 (1965).

¹⁰ W. van Roosbroeck and W. Shockley, *Phys. Rev.* **94**, 1558 (1954).

¹¹ P. T. Landsberg and T. S. Moss, *Proc. Phys. Soc. (London)* **B69**, 661 (1956).

¹² R. N. Zitter, A. J. Strauss, and A. E. Attard, *Phys. Rev.* **115**, 266 (1959).

¹³ H. Y. Fan and R. A. Laff, *Phys. Rev.* **121**, 53 (1961).

direct band-to-band transitions, and band-to-flaw transitions. Also detected were narrow, low-level lines having energies equal to and greater than the band gap. In the results section, these observations are presented and identification of most of those lines greater than kT in width are made. The room-temperature emission is compared with statistical theory and the room-temperature bulk to radiative lifetime ratio determined from the total emission. The energy levels of several impurities in InSb are determined from the low-temperature data. The emission from a highly doped specimen is compared with photon distribution calculations of the possible radiative recombination processes. In the discussion, our results and those of Guillaume and Lavallard, which differ in some respects, are compared. Some observations of the nature of the fine structure lines are also included.

EXPERIMENTAL PROCEDURE

The generation of excess carrier populations in InSb single crystals was accomplished by optical injection. Chopped radiation from a high-intensity arc source was focused onto the surface of thick single-crystal specimens. The radiation emitted was collected and analyzed with a prism spectrophotometer. The source, a 300 W zirconium arc, was imaged onto the specimen with a spherical mirror such that the angle of incidence was approximately 45° . Radiation normal to the surface of the specimen was imaged onto the entrance slit of the spectrophotometer. Scattering of source radiation into the emission path was for the most part no problem. The combination of the glass envelope of the source and glass filters removed essentially all the scattered radiation beyond 3.2μ . The spectrophotometer was a slightly modified Model 12 Perkin-Elmer instrument. A Reeder radiation thermocouple with a KRS-5 window was used as the detecting element. The associated electronics consisted of a 13 cycle phase-sensitive Perkin-Elmer system in which RC of the dc end was substantially increased to a maximum value of almost four minutes. As a consequence the noise equivalent voltage of the system could be held to 10^{-10} V, which at maximum sensitivity was equivalent to 2×10^{-11} W input on the thermocouple. Because of the long response time, many of the data were obtained by point-by-point plotting. Resolutions of 10^{-3} eV were achieved. The wavelength range investigated was 3 to 35μ .

The specimens had surface dimensions of $1 \times \frac{1}{2}$ cm and were about $\frac{1}{2}$ cm thick. They were ground and polished, soldered to copper mounts for attachment to suitable cryostats, and etched electrolytically with a solution of eight parts ethylene glycol and one part nitric acid. Dilute HF was used as a rinse to remove large traces of residual oxide.

Thermocouples were used to measure the temperature at the surface of InSb crystals. Iron versus con-

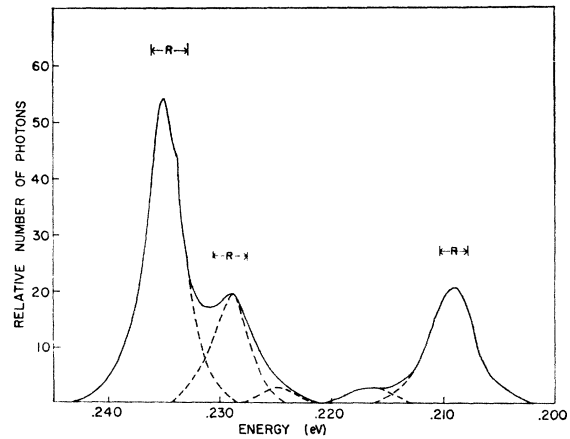


Fig. 1. Photon emission versus photon energy of silver-doped InSb at 12°K . ($N_A - N_D = 5 \times 10^{14}/\text{cc}$.)

stantan was used for temperatures above 77°K , and a gold- (2.1 at. % silver) versus copper thermocouple for temperatures below. To insure good thermal contact, the thermocouples were soldered to the surfaces of the specimens. The temperature of specimens was not measured at the time of an emission measurement in order to prevent any disturbance of the surface by the soldering. Temperature measurements were reasonably consistent for a particular coolant. The emission was measured for uncooled samples and for samples cooled with solid carbon dioxide, liquid nitrogen, and liquid helium. The temperatures recorded under these thermal conditions were 300, 200, 100, and 12°K , respectively.

The variation of the radiative emission with the intensity of the optical input was measured using a set of four grey filters placed between the arc source and the specimen.

Fourteen single-crystal specimens were investigated. The 77°K carrier concentrations of these varied from 5×10^{17} n type to 2×10^{15} p type. Of the p -type specimens, two were doped with zinc, three with silver (two with selenium compensation) and two with gold (one with selenium compensation). About half of the single crystals were grown at Syracuse; the rest were obtained from Cominco Products, Inc.

RESULTS

The general features of the radiative emission observed in this work are an emission line whose energy distribution lies for the most part at energies greater than the band-gap energy, narrow low-intensity emission lines superimposed on the above distribution, and emission at energies less than the band gap which at the lowest experimental temperature consisted of distinct spectral lines. These three distinct line groups are illustrated in Fig. 1, which presents the distribution of photons emitted from a p -type silver-doped single

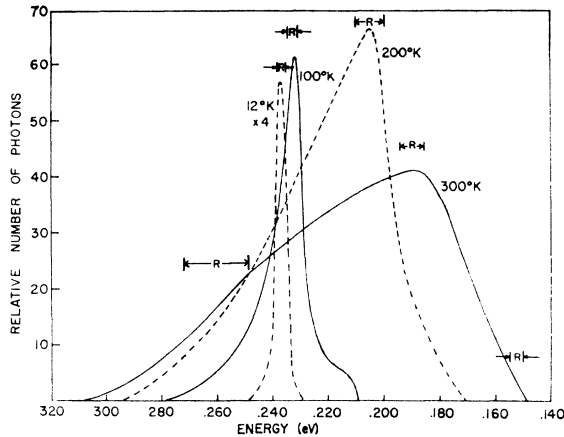


FIG. 2. Band-to-band radiative recombination at 12, 100, 200, and 300°K. ($n_0 = 10^{14}/\text{cc}$ at 77°K.)

crystal at 12°K. The emission is plotted against an arbitrary scale; however, the same scale is used in subsequent figures unless otherwise noted.

1. Band to Band Radiative Recombination

A. Direct

The broad ($>kT$) line which consists chiefly of photons having $h\nu > E_g$ was observed at the four experimental temperatures in some of the purer specimens, and from all specimens at 12°K. The peak magnitude of the line shifted to higher energies with decreasing temperature as shown in Fig. 2. The half-width was greater than kT , varying from about 8×10^{-2} at 300°K to 4×10^{-3} eV at 12°K. At 12°K in those crystals having impurity concentrations of $10^{15}/\text{cm}^3$ or less, the line peaked within the range 0.235 to 0.237 eV and at 300°K, at 0.189 eV. The energy values obtained by extrapolating the low-energy edge of the line to zero emission are 0.177 eV at 300°K, 0.196 eV at 200°K, 0.227 eV at 100°K, and 0.234 eV at 12°K. These values agree quite well with the band gap of InSb. Oscillatory magneto-absorption and reflection experiments fix the band gap at 0.180 eV at 300°K,¹⁴ 0.228 eV at 80°K,¹⁵ and 0.236 eV at 4°K.¹⁶ This agreement together with the other characteristics of the line establish that the photon output is primarily due to direct band-to-band (DBB) radiative transitions. The tailing off of this line below band-gap values is due either to a tailing of the density of states or indirect transitions.

The intensity of DBB radiation from p -type specimens at 12°K was, in general, less than that from n -type specimens, and tended to decrease with increas-

ing net acceptor concentration. This behavior is in accord with the asymmetric nature of the capture cross section for electrons and holes by those recombination centers in InSb^{12,13} which set the bulk recombination rate. However, the DBB radiative output from compensated silver- and gold-doped crystals was lower than that from the uncompensated crystals and other specimens which had higher net acceptor concentrations. Apparently, a significant increase of the capture rate of holes occurred as a result of the ionization by compensation of the deep acceptor levels of silver and gold.

Measurements of the variation of the peak magnitude of this emission line with the intensity of the input carrier-generating radiation for two n -type specimens gave the following results: at 300°K the variation was linear, whereas at 12 and 100°K, a substantial quadratic dependence was exhibited.

When nonradiative processes control the rate of excess-carrier recombination, the radiative rate relation is

$$\Delta R = \langle P \rangle [n_0 \Delta p + p_0 \Delta n + \Delta n \Delta p], \quad (1)$$

where $\langle P \rangle$ is the average radiative-recombination coefficient, n_0 and p_0 are the equilibrium electron and hole concentrations, and Δn and Δp are the excess-carrier concentrations. In n -type InSb specimens, whether the excess-carrier concentrations are controlled by band-to-band Auger recombination or by recombination through centers, $\Delta n \approx \Delta p$. Hence,

$$\Delta R = \langle P \rangle [(n_0 + p_0) \Delta n + \Delta n^2].$$

At room temperature the measured linear dependence is in accord with this relation. Consideration of the Auger lifetime and transport equations fix Δn well below n_0 at 300°K, which is $1.6 \times 10^{16}/\text{cm}^3$. At 12 and 100°K, the quadratic dependence indicates that $\Delta n > n_0$, and at least when the intensity of the DBB line was high that $\Delta n > 10^{14}/\text{cm}^3$ in the region close to the crystal surface.

At 300°K small-signal theory^{10,11} would be expected to apply. When $\Delta n = \Delta p$ and $n_0 = p_0$, the small-signal bulk generation rate is

$$\Delta R_B = (2R \Delta n) / n_0, \quad (2)$$

where R is the thermal equilibrium radiative rate. The expression for R is obtained by invoking detailed balance and can be written

$$R = 4 \int n(\lambda)^2 \alpha(\lambda) Q(\lambda) d\lambda, \quad (3)$$

where n is the index of refraction, α is the absorption coefficient, and Q is Planck's law of surface emission.

The excess carrier distribution generated by highly energetic radiation in a thick specimen will be depth-dependent, and furthermore the recombination radia-

¹⁴ S. Zwerdling, B. Lax, and L. M. Roth, Phys. Rev. **108**, 1402 (1957).

¹⁵ G. B. Wright and B. Lax, J. Appl. Phys. **32**, 2113 (1961).

¹⁶ S. Zwerdling, W. H. Kleiner, and J. P. Theriault, J. Appl. Phys. **32**, 2118 (1961).

tion will be attenuated by reabsorption. Hence, the radiation reaching the surface will be

$$\Delta r_s(\lambda) = \frac{2r(\lambda)}{n_0} \int_{\infty}^0 \Delta n(y) \exp[-\alpha(\lambda)y] dy, \quad (4)$$

where α is the total absorption coefficient. A calculation of the carrier concentration as a function of depth for the intrinsic case yields

$$\Delta n(y) = \frac{\alpha' I \tau}{\alpha'^2 L^2 - 1} \times \left[\left(\frac{L^2 \alpha' + s \tau}{L + s \tau} \right) \exp(-y/L) - \exp(-\alpha' y) \right] \quad (5)$$

if the following assumptions are made: small signals, one-dimensional flow, charge neutrality, no appreciable influence of charge trapping, and the effect upon the spatial distribution of carriers due to emitted radiation is small. α' is the band-to-band absorption coefficient at the wavelength of the incident radiation, I the incident photon flux, τ the lifetime of the free carriers, L the diffusion length, s the surface recombination velocity, and y the distance into the specimen from the surface.

For most of the input radiation, $\alpha' > 10^5 \text{ cm}^{-1}$, and at 300°K , $L \approx 4 \times 10^{-3} \text{ cm}$.¹⁷ Hence, when s is assumed to be much less than 10^5 cm/sec , the expression for the radiation reaching the surface per unit waveband simplifies to

$$\Delta r_s(\lambda) \approx \frac{8 n(\lambda)^2 \alpha'(\lambda) Q(\lambda) I \tau}{n_0 (1 + \alpha(\lambda) L)}. \quad (6)$$

In Fig. 3 this function is plotted versus wavelength for a constant value of the index of refraction together with the 300°K experimental curve which has been normalized to constant resolution in wavelength. A

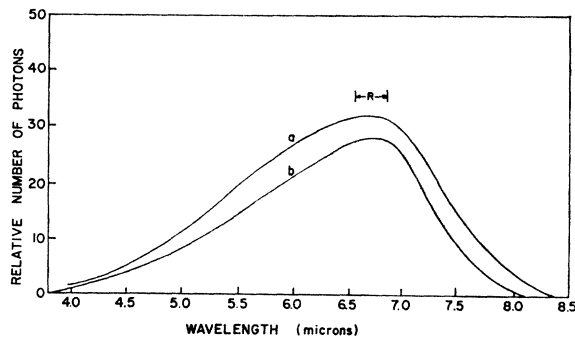


FIG. 3. Theoretical and experimental 300°K photon emission. (a) Experimental emission adjusted for constant λ resolution; (b) statistical theory.

¹⁷ D. G. Avery and D. P. Jenkins, J. Electron. 1, 145 (1955).

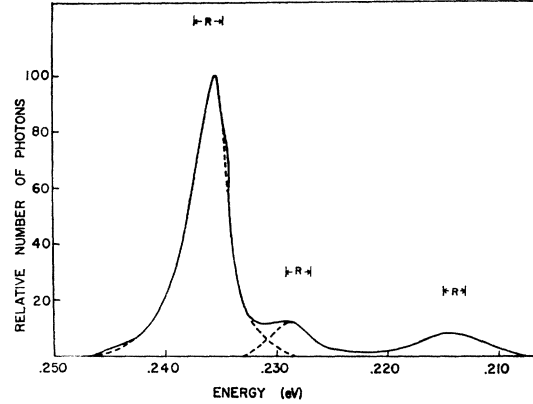


FIG. 4. Photon emission versus photon energy at 12°K . ($n_0 = 10^{14}/\text{cc}$ at 77°K .)

reasonably good fit exists between the measured and calculated emission. The absorption coefficient data used for the calculation of the bulk emission were those measured by Moss¹⁸ for an intrinsic crystal.

Following Moss,² from Eq. (6) the total radiative output can be expressed as

$$\Delta R_t \approx \frac{I \tau_B}{\tau_B} \times 10^{-2} \int \frac{\alpha' Q}{1 + \alpha L} d\lambda / \int \alpha' Q d\lambda. \quad (7)$$

The expression takes into account the fact that because of internal reflection only about one percent of the radiation reaching the surface leaves, and it also incorporates the relation for the radiative lifetime

$$\tau_R = n_0 / 2R.$$

ΔR_t can be obtained by integrating the experimentally determined emission distribution. The integrals on the right are evaluated from calculated curves. The value of I , the effective input photon flux, includes the emission of the arc source, the fraction of the source emission collected, the loss of the optical system, the percentage absorbed, the size of the source image, and an average generation quantum efficiency η . The source characteristics and optical parameters are known reasonably well while η is estimated to be 1.5 using Tauc's¹⁹ data and the spectral distribution of the source. The ratio τ_B/τ_R evaluated from Eq. (7) is 6.5×10^{-2} while the ratio of the measured bulk lifetime to calculated radiative lifetime obtained from the data of Zitter *et al.*,¹² is about 7×10^{-2} sec.

B. Indirect

The intensity of one of the emission lines less energetic than the band gap in the 12°K spectra had the same dependence upon input intensity as the DBB line. The line peaked at or close to 0.215 eV and was

¹⁸ T. S. Moss, Proc. Phys. Soc. (London) B70, 778 (1957).

¹⁹ J. Tauc, J. Phys. Chem. Solids 8, 219 (1959).

from ten to twenty times less intense than the DBB line. The emission shown in Fig. 4 is typical. The line is therefore tied to the populations of both bands just as an indirect band to band (IBB) transition would be. In InSb the energy of optical phonons at the center of the zone are longitudinal: 0.0244 eV,²⁰⁻²² and transverse: 0.0234 eV.²² On the other hand, the maximum energy of acoustical phonons, occurring at the zone edge, is 0.0196 eV.²² Since the electron and hole populations peak close to $\mathbf{k}=0$, the line is concluded to arise from indirect transitions in which an optical phonon is created.

For a line peaking at 0.215 eV, the addition of 0.024 eV, the optical phonon energy, gives a transition energy of 0.239 eV. This value represents the energy difference between the peaks of the electron and hole distributions. This knowledge together with band data^{23,24} makes possible an estimate of the density of excess electrons in the conduction band close to the surface, which is $2 \times 10^{15}/\text{cm}^3$ in this case.

At 100°K the indirect line should lie at about 0.213 eV for pure specimens. Presumably this line is part of the tail of the 100°K photon distribution which extends to 0.209 eV.

2. Radiative Recombination Through Flaws

Several emission lines were observed at 12°K which were less energetic than the band gap of InSb, had half-widths greater than kT , and varied in intensity directly with the input radiation flux. These lines therefore appear to be due to band-to-flaw transitions.

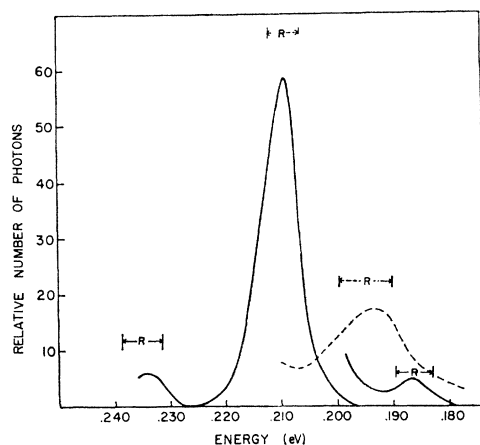


FIG. 5. Photon emission versus photon energy of compensated silver and gold-doped InSb. (—) Ag+Se ($n_0=9 \times 10^{12}$ at 77°K); (---) Au+Se ($n_0=1 \times 10^{14}$ at 77°K).

²⁰ W. Engeler, H. Levinstein, and C. Stannard, Jr., Phys. Rev. Letters 7, 62 (1961).

²¹ R. N. Hall, J. H. Racette, and H. Ehrenreich, Phys. Rev. Letters 4, 459 (1960).

²² S. J. Fray, F. A. Johnson, and R. H. Jones, Proc. Phys. Soc. (London) 76, 939 (1960).

²³ S. D. Smith, T. S. Moss, and K. W. Taylor, J. Phys. Chem. Soc. 11, 131 (1959).

²⁴ G. W. Gobeli and H. Y. Fan, Phys. Rev. 119, 613 (1960).

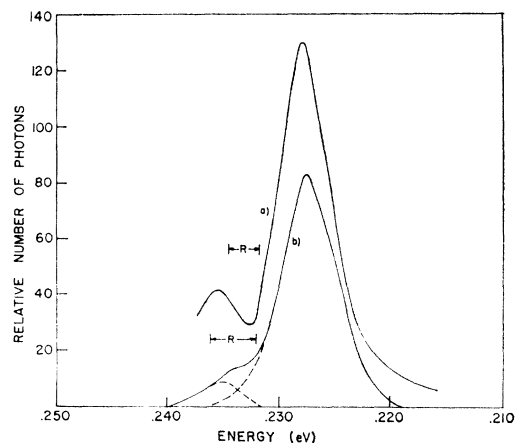


FIG. 6. Photon emission versus photon energy of Zn-doped InSb at $T=12^\circ\text{K}$. (a) $p_0=2 \times 10^{14}/\text{cc}$ at 77°K; (b) $p_0=2 \times 10^{15}/\text{cc}$ at 77°K.

Crystals doped with silver and gold yielded lines which were directly associated with the presence of these impurities. In silver-doped crystals, two lines were observed peaking at 0.2090 and 0.1865 eV, the latter being much weaker than the former. In specimens doped with gold, only one line, peaking at 0.1928 eV, could be detected, and it was much weaker than the first silver line. These lines are shown in Fig. 5.

The flaw line which appeared most frequently in the emission spectra (from seven specimens) peaked in the energy range 0.2275 to 0.2288 eV. In the purest crystal in which this line was detected ($n_0=1 \times 10^{14}/\text{cm}^3$ at 77°K) the line peaked at 0.2283 ± 0.0003 eV on the basis of five measurements. The line, however, was most intense when emitted by a crystal deliberately doped with zinc such that $p_0=2 \times 10^{14}/\text{cm}^3$ at 77°K. The same emission line from a crystal having a higher concentration of zinc ($p_0=2 \times 10^{15}/\text{cm}^3$ at 77°K) was not as great; however, the ratio of the intensity of this flaw line to the DBB line 10 was considerably greater than that for other specimens. With the other zinc-doped specimen it was 2.8, while in those remaining specimens which yielded a detectable 0.228 eV line the ratio ranged from 0.05 to 1.6. The emission from the zinc-doped crystals is shown in Fig. 6. It therefore appears that this line is due to radiative transitions from the conduction band to the low-lying zinc acceptor level, or levels produced by impurities of the same class, e.g., cadmium. Both zinc and cadmium have high segregation coefficients in InSb. A line at 0.228 eV is also prominent in the emission spectra of a variety of n - and p -type InSb crystals, observed by Mooradian and Fan.³

According to effective-mass theory²⁵ and following Eagles,²⁶ the matrix element for a direct band to

²⁵ W. Kohn, *Solid State Physics*, edited by F. Seitz and D. Turnbull (Academic Press Inc., New York, 1957), Vol. 5, p. 257.

²⁶ D. M. Eagles, J. Phys. Chem. Solids 16, 76 (1960).

shallow level transition should be principally dependent upon a wave-dependent coefficient which is a Fourier transform of a hydrogen-like function, i.e.,

$$|M_i| \propto a(\mathbf{k}) |M_0| \propto \frac{1}{[k^2 + (1/a^{*2})]^2} |M_0|. \quad (8)$$

M_0 is the band-to-band matrix element which is a slowly varying function of energy. a^* , a modified Bohr radius, is given by $a^* = a_0 \epsilon (m_0/m^*)$, where a_0 is the Bohr radius, ϵ is the static dielectric constant, and m^*/m_0 is the effective mass ratio. In those specimens where n_0 at $77^\circ\text{K} \leq 10^{15}/\text{cm}^3$, the conduction band population peaked at no more than 0.004 eV above the band minimum, which corresponds to $k \approx 0.005$ atomic units (a. u.) Over this range of k , according to Eq. (8), the transition probability should vary little. Hence, the emission peak should accurately represent the population peak in the conduction band. The magnitude and shape of the flaw lines as a function of input intensity support this view.

The energy at which the conduction band population peaks can be estimated with reasonable accuracy from band, band-to-band line, and intensity data. Therefore, the energy of the impurity levels can be determined quite accurately from the energy of the related lines. For example, in the crystal where $p_0 = 1 \times 10^{14}/\text{cm}^3$ at 77°K , the zinc line peaked at 0.228 eV while the conduction band population peaked at about 0.238 eV above the valence band maximum. Consequently, a mean ionization energy of 0.010 eV is indicated for zinc atoms at low concentrations. The energies of the zinc level in the crystals doped with zinc such that $p_0 = 2 \times 10^{14}/\text{cm}^3$ and $2 \times 10^{15}/\text{cm}^3$ at 77°K are determined to be 0.0082 and 0.0075 eV, respectively. These values are in decent agreement with the concentration dependence of the ionization energy of a shallow acceptor determined from Hall data,^{27,28} which is $E = \epsilon_0 - \beta N^{1/3}$, where ϵ_0 is between 9.4×10^{-3} to 9.8×10^{-3} eV and β is either 1.8×10^{-8} or 1.9×10^{-8} eV cm.

Since holes would be more tightly bound to silver and gold atoms than to group II impurity atoms, it is expected that the volume in reciprocal space within which the wave vector-dependent coefficients of the impurity wave functions are constant will be greater than for shallow states. Therefore the conduction band population should, as in the case for zinc, primarily determine the photon distribution arising from conduction band to deep level transitions. From an estimate of the energy at which the electron population is at a maximum, the energy of the two silver levels is determined to be 0.027 eV and 0.050 eV above the valence band, and the lower gold level to be 0.043 eV.

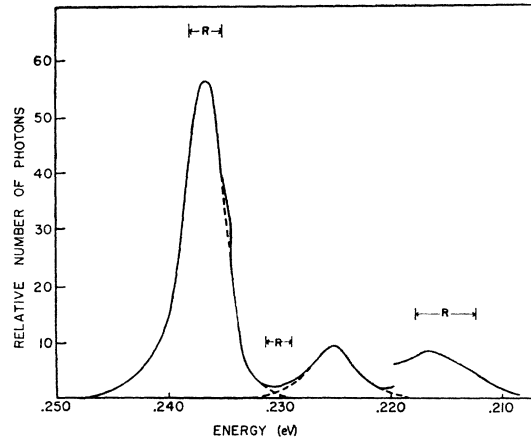


FIG. 7. Photon emission versus photon energy at 12°K . ($n_0 = 5.7 \times 10^{13}/\text{cc}$ at 77°K .)

The impurity ionization energies deduced from our data are compared with values determined in other ways in Table I.²⁹⁻³¹ The values quoted for zinc via

TABLE I. Energy levels of impurities in InSb obtained by different experiments.

Impurity	Emission $E_i - E_v$	Oscillatory photocon- ductivity $E_i - E_v$	Hall $E_i - E_v$	Photocon- ductivity $E_i - E_v$
Zn	0.010		0.008 ^b 0.010 ^c 0.010 ^d	
Ag I	0.027	0.028 ^a	0.023 ^d	
Ag II	0.050			0.039 ^e
Au I	0.043	0.043 ^a	0.032 ^d	

^a See Refs. 20 and 31.

^b See Ref. 29.

^c See Ref. 28.

^d See Ref. 30.

^e See Ref. 31.

Hall measurements are not specifically for zinc, but are thought to belong to one or more group II impurities.

One other flaw line was observed which peaked at 0.2250 eV (Fig. 7). It appeared distinctly in only one specimen which was probably the purest specimen ($n_0 = 6 \times 10^{13}/\text{cm}^3$ at 77°) of those studied. However, this line probably was present in the emission from some of the other specimens but may have been masked by the much more intense 0.228 eV line, as indicated in Fig. 1. From an estimate of the excess carrier distribution the level is determined to be either 0.012 eV above the valence band or 0.010 eV below the conduction band. Since the line appeared most

²⁷ W. Engeler, Doctoral dissertation, Syracuse University, 1961 (unpublished).

²⁸ R. F. Broom and A. C. Rose-Innes, Proc. Phys. Soc. (London) **B69**, 1269 (1956).

²⁹ E. H. Putley, Proc. Phys. Soc. (London) **73**, 128 (1959).

³⁰ W. Engeler and H. Levinstein, Bull. Am. Phys. Soc. **6**, 156 (1961).

³¹ W. Engeler, H. Levinstein, and C. R. Stannard, Jr., J. Phys. Chem. Solids **22**, 249 (1961).

strongly in the purest crystal studied, the level is concluded to be associated with a structural defect. No other lines were observed out to 35 μ .

3. Radiative Recombination in Highly Impure Crystals

The 12°K recombination radiation spectrum of the most heavily doped specimen studied (tellurium doped such that $N_D - N_A \approx 5 \times 10^{17}/\text{cm}^3$) consisted primarily of a line that was much broader than the emission lines of purer specimens. The breadth is a consequence of the fact that complete filling of a considerable portion of the conduction band by electrons from shallow donors occurs at moderate concentrations in InSb. The line had a half-width of 0.06 eV and from one (211) face it peaked at 0.297 eV and at 0.314 eV from the other. The difference in the energy of the peak of the lines from opposite surfaces is presumably due to a substantial variation in excess donor concentration within the specimen. The smoothed photon distribution from one of the surfaces obtained by varying the slit width to maintain constant resolution and adjusting the magnitude accordingly is shown in Fig. 8. Figure 9 illustrates the emission from an opposite surface of the same specimen recorded at constant slit width. The large dip at 0.29 eV is due to absorption by atmospheric CO₂. Also included in the emission from this highly degenerate specimen is an additional emission component at the low-energy end of the main photon distribution as shown in Figs. 8 and 9. This component, which begins at 0.211 eV, has the form of a low-intensity emission line that overlaps the broad emission distribution, and which peaks at about the same energy as the extrapolated edge of the broad emission line (0.222 eV).

The radiation that is generated by transitions from completely occupied states will be unabsorbed. Therefore the emission spectrum should accurately reflect the density-of-states function and the occupation and transition probabilities associated with these radiative transitions, and should permit direct comparison with calculated bulk emission distributions.

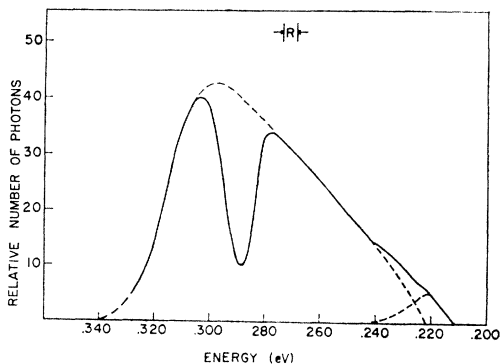


FIG. 8. Photon emission versus photon energy for constant resolution at 12°K. ($n_0 \approx 4.8 \times 10^{17}/\text{cc}$ at 77°K.)

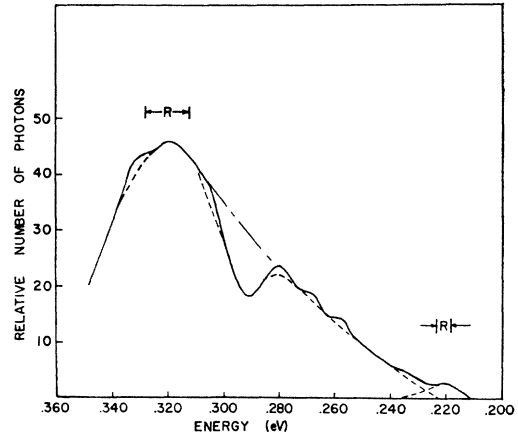


FIG. 9. Photon energy versus photon emission at 12°K. ($n_0 \approx 4.8 \times 10^{17}/\text{cc}$ at 77°K.)

Four first-order radiative recombination processes are considered for comparison with the experimental observation. These are band-to-band and band-to-shallow flaw transitions with and without \mathbf{k} conservation. Because of the appreciable interaction of impurity states with band states, \mathbf{k} conservation may not be required.

The DBB transition spectral distribution obtained from conventional transition theory in which \mathbf{k} conservation is invoked, assuming spherical bands, is³²

$$\Delta r(h\nu) \propto h\nu |M_0(h\nu)|^2 \rho(h\nu) f_c(E') f_v(E''), \quad (9)$$

where M_0 is the matrix element for the transition, $\rho(h\nu)$ is the composite conduction and valence band density-of-states for the transition $h\nu$, and $f_c(E')$ and $f_v(E'')$ are the occupation probabilities of electrons in the conduction band and holes in the valence band for states separated by $h\nu$ but having the same \mathbf{k} . The occupation probabilities in the energy range where the conduction band is filled are $f_c(E') = 1$ and $f_v(E'') \propto \exp[(E'' - E_f'')/kT]$,³³ hence within this range

$$\Delta r(h\nu) \propto h\nu |M_0(h\nu)|^2 \exp[(E'' - E_f'')/kT]. \quad (10)$$

When \mathbf{k} conservation is not required the general relation for the band-to-band spectral distribution will be

$$\begin{aligned} \Delta r(h\nu) \propto h\nu \int \int_{\mathbf{v}} |M_0(E' - E'')|^2 \\ \times \rho_c(E' - E_c) f_c(E_f' - E') \rho_v(E_v - E'') f_v(E'' - E_f'') \\ \times \delta(h\nu - E' + E'') dE' dE''. \quad (11) \end{aligned}$$

Since in InSb, $\rho_v \propto (E_v - E'')^{1/2}$,²⁴ the spectral emission at energies in which conduction band states are filled

³² For a detailed treatment of direct radiative recombination, \mathbf{k} and non- \mathbf{k} conserving, see G. Lasher and F. Stern, Phys. Rev. 133, A553 (1964).

³³ The magnitude of the emission indicates that the hole population is nondegenerate.

becomes

$$\Delta r(h\nu) \propto h\nu \int_0^{h\nu - E_g} |M_0(h\nu)|^2 \rho_c(E) (h\nu - E_g - E)^{1/2} \times \exp\left(\frac{E + E_c - h\nu - E_f''}{kT}\right) dE. \quad (12)$$

For a band-to-shallow flaw transition which conserves crystal momentum the spectral distribution due to transitions from filled band states to a discrete level is just

$$\Delta r(h\nu) \propto h\nu |M_s(h\nu)|^2 \rho_c(h\nu). \quad (13)$$

The matrix element predicted by effective mass theory for simple bands is given by Eq. (8). When the \mathbf{k} selection rule does not apply, the band-to-shallow flaw emission distribution will be given by the summation of all transitions which yield photons of energy $h\nu$, i.e., Eq. (13) is summed over \mathbf{k} .

These expressions were evaluated using the band-to-band matrix element calculated by Kane³⁴ and the conduction band density-of-states function obtained from Faraday effect²³ and optical absorption²⁴ data. Since the conduction band effective mass is very much less than that of the heavy hole band, the choice of the heavy hole mass has a negligible influence on the shape of the composite density-of-states function. The calculated curves are compared in Fig. 10 with that portion of the experimental curve below the intensity peak (0.242 to 0.287 eV) that appears to be uninfluenced by the extra low-energy emission component as indicated by the curves of Figs. 8 and 9.

The calculated band-to-band, \mathbf{k} -conserving distribution peaks at about 0.24 eV and drops off slowly beyond (Fig. 10, curve b). In contrast, the experimental distribution (a) peaks at about 0.296 eV followed by a sharp drop off. On the other hand, the calculated non- \mathbf{k} conserving band-to-band and band-to-shallow flaw radiative distributions have the general shape of the experimental curve, i.e., they peak at a high-energy value (representative of the Fermi level in the conduction band) and drop off rapidly beyond.

For a constant transition matrix element the rate relations for band-to-flaw and the non- \mathbf{k} conserving band-to-band transitions are essentially equivalent. The value of the integral in the non- \mathbf{k} conserving band-to-band relation is primarily only dependent upon the conduction band density-of-states function within the energy range of interest. When normalized at 0.242 eV, the curve (c) representative of these cases lies substantially above the experimental curve. However, when the values of the matrix element calculated by Kane³⁴ are taken as the average value for a transition energy $h\nu$, the curve for non- \mathbf{k} conserving transitions

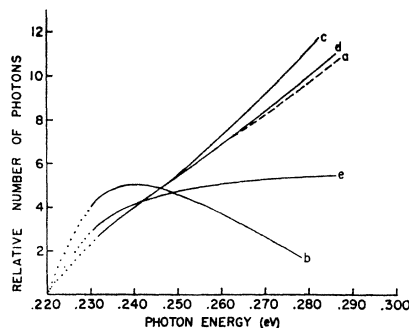


FIG. 10. Calculated and experimental emission distributions for filled conduction band. (a), Experimental curve ($n_0 \approx 4.8 \times 10^{17}/\text{cc}$ at 77°K); (b), Band-to-band, \mathbf{k} conservation; (c), Band-to-band, non- \mathbf{k} conservation and band-to-shallow flaw; constant transition matrix element; (d), Band-to-band and band-to-shallow flaw, non- \mathbf{k} conservation; Kane's matrix element; (e), Band-to-shallow flaw, \mathbf{k} conservation.

(d) comes close to fitting the experimental phonon distribution. On the other hand, when the effective mass matrix element Eq. (8) is incorporated in the \mathbf{k} conserving band to shallow flaw relation, the calculated distribution (e) falls much below the experimental curve. For this calculation the valence band effective mass was taken as $0.25 m_0$. Even for $m_h^* = 0.60 m_0$ (values ranging from $0.18 m_0$ to $0.60 m_0$ have been reported in the literature) the curve calculated from Eqs. (13) and (8) would still fall considerably below that observed.

The good fit of the calculated non- \mathbf{k} conserving curve with the experimental curve suggests that non-conserving band-to-band or band-to-shallow flaw transitions account for the emission from the very impure crystal. However, \mathbf{k} -conserving band to shallow flaw transitions could be the dominant radiative process should the transition probability nearly be a constant within the energy range of the experiment.

Regardless of which of these cases is dominant, the experimental curve of Fig. 8 probably gives a close representation of the distribution of conduction band states with energy since the product $h\nu |M_0|^2 \approx$ constant. On this basis, the departure from smoothness at the low-energy end is due to a variation of the density-of-states produced by the impurity-conduction band interaction.

The distribution of photons emitted by this crystal indicates that in addition to extension of the conduction band by the donor-state interaction, a decrease of the band gap also occurs because of a shift of the bands. A difference of 0.012 eV exists between the extrapolated impure and pure InSb edge energies, and may be indicative of the magnitude of the shift. However, if band-to-flaw transitions account for the observed emission then the shift of bands could be substantially less than this value. According to results discussed earlier, the flaw that would most likely be a strong radiative recombination center in InSb crys-

³⁴ E. O. Kane, J. Phys. Chem. Solids 1, 249 (1957).

tals is a shallow acceptor with an effective ionization energy of 0.010 eV or less, depending upon concentration. Hence, if the primary radiative recombination is to these ionized acceptors, the shift of the bands could be as little as 0.002 eV.

4. Fine Structure

At 12 and 100°K consistent departures from smoothness of the emission were observed at energies equal to and greater than the band gap. These variations had the appearance of narrow, low-intensity emission lines superimposed upon the broader, more intense emission line which results from recombination of carriers in the conduction band. In general these narrow lines were quite weak, being not much greater than system noise. The half-width of these lines were resolution limited. Figures 4, 9, and 11 illustrate the existence of these lines at the two temperatures. At 100°K several lines were in evidence, and consistently appeared in all specimens where DBB emission was appreciable. At 12°K one or two lines appeared in *n*-type specimens having an impurity concentration of $10^{16}/\text{cm}^3$ or less and in several *p*-type specimens. The 12°K emission of the *n*-type crystal with largest excess-donor concentrations, $N_D - N_A \approx 5 \times 10^{17}/\text{cm}^3$, exhibited a greater number of these lines. The fine structure emission lines observed from a given specimen were independent of etching. The same energy configuration was obtained each time new surfaces were formed. Identical results were likewise obtained for opposite surfaces.

The spectrometer, reflected radiation, and atmospheric characteristics were carefully checked to determine if one of these were the sources of the recorded structure. No evidence of their influence could be detected. The characteristics of these lines eliminate an interference effect as a possibility.

Tables II and III present the energy values of the fine structure lines at 12 and 100°K, respectively. A striking feature of the spectra at 100°K is that the

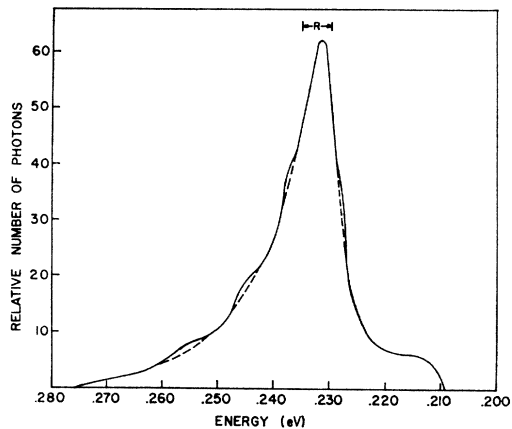


FIG. 11. Photon energy versus photon emission at 100°K. ($n_0 = 1.6 \times 10^{14}/\text{cc}$ at 77°K.)

TABLE II. Fine structure energy values at 12°K.

Type	Carrier conc. cm^{-3} at 77°K	Energy of fine structure lines (eV)
<i>n</i>	1×10^{14}	0.2445; 0.2343 0.2449; 0.2337 0.2443 0.2450
<i>n</i>	1.6×10^{14}	0.245; 0.2338 0.2465; 0.2342 0.245
<i>n</i>	5.7×10^{13}	0.234 0.246
<i>p</i>	3×10^{13}	0.2343
<i>p</i>	5×10^{14} *	0.235
<i>p</i>	1×10^{15}	0.234
<i>n</i>	1×10^{16}	0.243
<i>n</i>	4.8×10^{17}	0.258; 0.269; 0.281; 0.306; 0.332 0.256; 0.267; 0.279; 0.304; 0.330

* $N_A - N_D$.

lines are equi-energy spaced within experimental error. Furthermore, there is a difference in the energy values between *n*- and *p*-type specimens, and the spacing appears to be slightly different, 0.009 eV for *n*-type specimens and 0.010 eV for *p*-type. At 12°K, *n*-type specimens exhibited up to two lines which were separated by 0.011 eV (0.234 and 0.245 eV), whereas, with *p*-type crystals, only one line was detected at 0.234 eV. Therefore, it appears that, for relatively pure specimens, the separation in energy of these lines, which start at about the band gap energy, are slightly dependent upon temperature and impurity type.

The 12°K fine structure spectra of the most impure specimen studied consisted of five reproducible lines. The energy separations of these lines, beginning at the lowest energy line (0.257 ± 0.001 eV), are 0.011, 0.012, 0.025, and 0.026 eV. The separation of the two lowest energy lines is equal to the energy separation between the two lines of the fine structure spectra of relatively pure *n*-type specimens. On the basis of the energies of these lines and those in purer specimens, one might expect that lines should also occur at energies below that of the first line separated by about 0.011 eV, and possibly between the third and fourth, and fourth and fifth lines. Then a set of lines would exist, separated in a systematic way, i.e., the energy separation would just increase slowly with energy. However, if other lines did exist forming such a set, they would have had to be considerably less intense than those observed.

TABLE III. Fine structure energy values at 100°K.

Type	Carrier conc. cm^{-3} at 77°K	Average energy of fine structure lines (eV)*
<i>n</i>	1×10^{14}	0.255 (3); 0.246 (5); 0.237 (5); 0.228 (3)
<i>n</i>	1.6×10^{14}	0.254 (2); 0.245 (2); 0.237 (5); 0.229 (1)
<i>p</i>	3×10^{13}	0.250 (2); 0.240 (2); 0.230 (2)
<i>p</i>	2×10^{14}	0.251 (1); 0.239 (1); 0.229 (1)

* Numbers in parentheses denote the number of separate measurements of the particular line.

A feature of the fine structure lines is that, although some variation in their magnitude was apparent, they did not vary in intensity as strongly as the band-to-band emission distribution. Lines occurring where the band-to-band emission was low were almost as distinct as those in the high emission region. Also, in pure specimens the fine structure and the DBB emission appeared to be influenced to approximately the same degree by a variation of input optical intensity. On the other hand, the magnitude of the lines existing in the spectrum from the highly degenerate n -type specimen were uninfluenced by a 50% decrease in the intensity of the input radiation, although the broad band-to-flaw emission decreased in proportion to the input. Evidently, the fine structure intensity is related to the occupation of conduction band states.

DISCUSSION

The energy distribution of the 300°K emission from thick intrinsic InSb crystals, which arises primarily from direct band-to-band transitions, agrees quite well with small-signal theory. There also is good agreement between the 300°K bulk to radiative lifetime ratio, 6.5×10^{-2} , obtained from the emission data, and the value obtained by using an experimental value of the bulk lifetime and a calculated one for the radiative lifetime. The energy of stimulated emission lines^{6,7} from InSb diodes at low temperatures compares favorably with the energy of the direct band-to-band spontaneous radiative recombination line we observed from single crystals at 12°K.

Comparison of the low-temperature spontaneous emission observed by Guillaume and Lavallard¹ (GL) from p - n structures with our observations reveals several differences. A line observed by them at 0.200 eV which had the characteristics of a band-to-band transition was attributed to an indirect, double optical phonon interaction. We did not observe this line, but rather one at 0.215 eV having similar characteristics. The 0.215-eV line agrees very well with the hypothesis of single optical phonon creation by an indirect transition when the $k=0$ energy of InSb optical phonons, ≈ 0.24 eV, is chosen as the phonon energy. GL also observed two lines, presumably associated with flaws, peaking at 0.2306 and 0.2165 eV. In a number of undoped specimens we similarly observed two lines having characteristics of band to flaw transitions but which peaked at 0.2284 and 0.2250 eV. The 0.2284 eV line, which appears to be related to zinc concentration in zinc-doped specimens, yields an acceptor-ionization energy, 0.010 eV for low-impurity concentrations, that is in very good agreement with Hall data for certain shallow acceptors. An emission line at 0.228 eV was also observed by Mooradian and Fan.³ A third difference concerns the emission from highly degenerate specimens. For an n -type specimen having a donor concentration of $2 \times 10^{17}/\text{cm}^3$, GL obtained a broad line that

started at 0.194 eV. With a specimen which had an excess donor concentration of about $5 \times 10^{17}/\text{cm}^3$ we observed a broad line beginning at 0.211 eV and peaking at 0.298 eV. In both cases a gap reduction due to impurity effects is indicated; however, the apparent shrinkage is considerably less when deduced from our data than from the data of GL.

Additional impurity lines were present in the emission spectra of silver- and gold-doped crystals. The ionization energies associated with these impurities as deduced from our data are 0.027 and 0.050 eV above the valence band for silver, and 0.043 eV above the valence band for the first gold level. The energies of the silver and gold levels agree very well with those deduced from oscillatory photoconductivity.^{20,31}

The observation of narrow emission lines ($< kT$ in width) equivalent to those we have observed in InSb, i.e., at energies greater than the band gap, has not been reported in the literature to our knowledge. Although narrow linewidth radiation has been observed in semiconductors, the energy of these lines has been less than the band gap by an amount equal to or greater than the free-exciton binding energy. These lines are a result of the decay of free excitons,^{35,36} excitons bound to single flaws,³⁶⁻⁴⁴ and transitions between electrons and holes bound separately to impurity atoms.⁴⁵⁻⁴⁸

Oscillatory optical absorption and emission in semiconductors and insulators due to Stark splitting of band states is predicted by Callaway.⁴⁹ The high electric field necessary to produce a substantial modulation of band states could conceivably exist at the surface of an InSb crystal because of band bending, and therefore as in this experiment where the excess carrier distribution for the most part is close to the crystal surface, the recombination radiation could exhibit an oscillatory characteristic. However, the sharpness of the lines we observe appears to eliminate tran-

³⁵ W. J. Turner, W. E. Reese, and G. D. Pettit, *Phys. Rev.* **136**, A1467 (1964).

³⁶ M. I. Nathan and G. Burns, *Phys. Rev.* **129**, 125 (1963).

³⁷ J. R. Haynes, *Phys. Rev. Letters* **4**, 361 (1960).

³⁸ C. Benoit a la Guillaume and O. Parodi, *Proceedings of the International Conference on Semiconductor Physics, Prague* (Czechoslovakia Academy of Sciences, Prague, 1961), p. 426.

³⁹ W. J. Choyke and L. Patrick, *Phys. Rev.* **127**, 1868 (1962).

⁴⁰ D. G. Thomas and J. J. Hopfield, *Phys. Rev.* **116**, 573 (1959).

⁴¹ D. G. Thomas and J. J. Hopfield, *Phys. Rev. Letters* **7**, 316 (1961).

⁴² D. G. Thomas and J. J. Hopfield, *Phys. Rev.* **128**, 2135 (1962).

⁴³ R. E. Halsted, M. R. Lorenz, and B. Segall, *J. Phys. Chem. Solids* **22**, 109 (1962).

⁴⁴ D. G. Thomas, M. Gershenson, and J. J. Hopfield, *Phys. Rev.* **131**, 2397 (1963).

⁴⁵ E. F. Apple and F. E. Williams, *J. Electrochem. Soc.* **106**, 224 (1959).

⁴⁶ J. S. Peneer and F. E. Williams, *Phys. Rev.* **101**, 1427 (1956).

⁴⁷ J. J. Hopfield, D. G. Thomas, and M. Gershenson, *Phys. Rev. Letters* **10**, 162 (1963).

⁴⁸ D. G. Thomas, M. Gershenson, and F. A. Trumbore, *Phys. Rev.* **133**, A269 (1964).

⁴⁹ J. Callaway, *Phys. Rev.* **130**, 549 (1963); **134**, A998 (1964).

sitions in which the continuum of band states participates or which are coupled to the lattice. Hence it appears that bound states exist in InSb, with energies that fall within the range of the continuum of band states. Such states would be quite different from those involved in the previously observed narrow emission spectra of semiconductors. The existence in silicon⁵⁰ and GaSb⁵¹ of bound states with energies that fall within the energy range of band states is indicated by experimental data. These are deduced to be impurity states associated with subsidiary band minima. Although similar states may exist in InSb, the characteristics of the sharp lines we have observed do not lead to the belief that such states are active in the observed transitions. The nature of the states involved in the transitions is not known. A number of states exist, the

⁵⁰ S. Zwerdling, K. J. Button, B. Lax, and L. M. Roth, *Phys. Rev. Letters* **4**, 173 (1960).

⁵¹ R. T. Bate, *J. Appl. Phys.* **33**, 26 (1962).

energy separation of which, within the energy range of the experiment, diverges with increasing energy. The data indicate that the intensity of the lines is to a large degree tied to the occupation of conduction band states. Hence, states at energies within the conduction band continuum are active in the decay process. Further, the energy of the associated optical transitions appears to be dependent upon temperature and somewhat related to the type of major impurity in the InSb crystals.

ACKNOWLEDGMENTS

We wish to thank Dr. H. Kaplan for an informative discussion with one of us regarding transition theory. Thanks are also due Dr. W. Engeler and Dr. C. Stannard, Jr., for their help. We are also indebted to J. Wrobel for growing many of the single crystals used in this study, and to K. Stannard and P. Lovecchio for technical assistance.

Nodal Hydrogenic Wave Functions of Donors on Semiconductor Surfaces*

JULES D. LEVINE

RCA Laboratories, Princeton, New Jersey

(Received 27 May 1965)

Quantum-mechanical properties have been derived theoretically for an isolated donor atom located at the surface of any dielectric crystal. The idealized surface potential is chosen to be $V = -e^2/\kappa r$ inside the dielectric and $V = +\infty$ outside, where e is the electronic charge, r is the radius from the donor-ion core, and κ is the dielectric constant of the crystal. V is chosen to be $+\infty$ outside the crystal because the valence electron is energetically more stable inside the crystal because of its high electron affinity. By using this potential, not previously used, the allowed wave functions are shown to be those hydrogenic wave functions which possess planar nodes. They have (1) the selection rule $l+m = \text{odd}$, (2) finite dipole moments, (3) l -shell degeneracy of l , (4) n -shell degeneracy of $n(n-1)$, and (5) unusual optical-polarization properties. The surface-donor ground state consists of one lobe of a $2p$ wave function; its ionization energy is only $\frac{1}{4}$ that of a bulk donor; and its dipole moment is 9.54κ Debye units.

I. INTRODUCTION

A DONOR atom located on a semiconductor surface will have properties considerably different from a donor atom located in the semiconductor bulk. Three examples of surface donors are: a phosphorus atom located on a silicon surface, a cesium atom on a sodium chloride surface, and a cesium atom on a sapphire surface. An understanding of surface-donor properties is important to adsorption physics, to catalysis, to thin-film formation, and to certain electronic devices dominated by surface effects. Also, the quantum-

mechanical properties associated with the chosen donor potential are simple and elegant.

A surface-donor atom is considered to be an ion core plus a valence electron moving about it in an atomic orbital, in accordance with quantum mechanics. Such a condition will prevail at low temperatures and is the condition of interest. At high temperatures the donor may become ionized whereby the valence electron moves in the crystal conduction band and Poisson's equation and Fermi-Dirac statistics must be used. We consider only the electronic structure of an isolated surface-donor atom before ionization.

Many workers¹⁻³ have attempted to calculate surface

* The research reported here was sponsored by the National Aeronautics and Space Administration, Lewis Research Center, Cleveland, Ohio, under Contract No. NAS 3-4173 and by RCA Laboratories, Princeton, New Jersey.

¹ J. Koutecky, *Trans. Faraday Soc.* **51**, 1038 (1958); *J. Surface Science* **1**, 280 (1964).

² T. B. Grimley, *J. Phys. Chem. Solids* **14**, 227 (1960).

³ T. A. Hoffman, *Acta Phys. Acad. Sci. Hung.* **2**, 195 (1952).